INTERNATIONAL CONFERENCE ON ENGINEERING DESIGN, ICED'09
24 - 27 AUGUST 2009, STANFORD UNIVERSITY, STANFORD, CA, USA

AN INTEGRATED CASE STUDY OF MATERIAL SELECTION, TESTING AND OPTIMIZATION

Martin Leary[1], Maciej Mazur[1], Roger Lumley[2] and Aleksandar Subic[1]
(1) RMIT University, School of Aerospace, Mechanical and Manufacturing Engineering, Australia (2) CSIRO Light Metals Flagship, Australia

ABSTRACT
An opportunity for design improvement through material substitution was identified by experimental assessment of an existing linear actuator. Material selection procedures were used to screen a broad database of materials to identify feasible candidates and quantify their relative merit. Further assessment by numerical methods identified additional opportunities for topological optimisation. Aluminum provides a compromise between the objectives of mass and cost and may provide an opportunity for enhanced material selection.
A novel process allows heat treatment of cast high pressure diecast (HPDC) aluminum alloys. The increased yield strength provides significant mass reduction opportunities.
Traditional material selection tools engage with a large number of candidate materials, but provide little design guidance for the optimisation of a specific scenario. Conversely, numerical optimization provides insight into specific scenarios, but has significant computational cost. The techniques applied in this paper provide an example of the integration of both methods; i.e. a course filter rapidly screens a large database, resulting in a subset that can be processed by the numerical methods within available design time.

Keywords: Material selection, light alloys, high-pressure die casting, optimisation

1 MATERIAL SELECTION
The feasibility and performance of a material for a specific design scenario may be directly evaluated from the constraints and objectives associated with the design specification [1]. Design constraints lead to material property limits that screen feasible materials according to the associated material properties. Design objectives lead to ratios of material properties, known as material selection indices, that rank the performance of a material for a given objective. Screening a group of candidate materials by the associated material property limits, and ranking the feasible materials by the material selection indices allows identification of the optimal material(s) for a specific design scenario [2].

1.1 Material property limits
Design constraints restrict the range of acceptable material properties, thereby providing a screening mechanism that identifies materials that are feasible for the design specification. Constraints of importance typically include limits on allowable: cost, design-duty, spatial envelope and deflection.

1.2 Material selection indices
Component performance, P, may be fully defined by a specific combination of material properties, defined as the *material index*, M^* [2]. The material index, M^*, has been defined such that performance is proportional to the associated material index. Material selection indices provide a powerful design tool for guiding material selection for a given design scenario, allowing the identification of the material properties relevant to performance, definition of the relative importance of these material properties, and performance comparison of specific materials. For relevant material properties, α and β, the general form of the material indices of interest to this work is (Table 1.):

$$M^* = \left(\frac{\alpha}{\beta^{1/k}} \right) = C \tag{1}$$

Where each value of the material index, C, defines a locus of constant performance. When plotted on a log-log chart of the relevant material properties, the locus of constant performance forms a linear *selection guideline* [3], with gradient, k (Equation 1). The selection guideline is a powerful tool for systematic material selection as (Figure 1):

- Performance is constant at any point along a selection guideline, for example, the performance at point A is equal to that of point A'.
- For a family of selection guidelines, performance is proportional to C, e.g. the performance of point A (or A') is greater than the performance at point B (or B'). When applying the selection guidelines relevant to the applications reported in this paper, performance is maximized toward the upper left hand side of the material property chart.

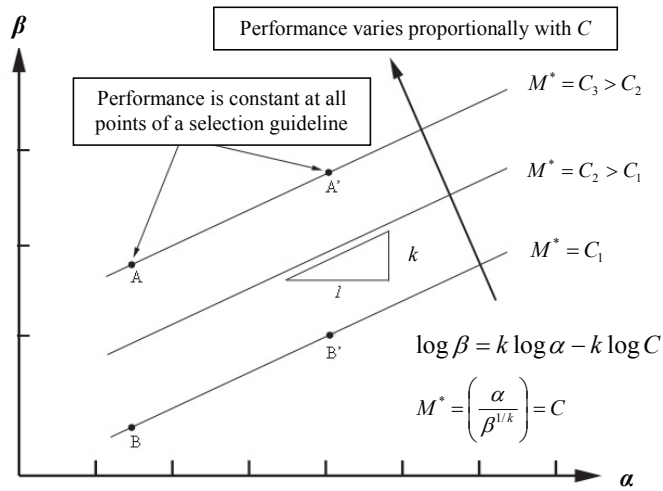

Figure 1. A generic material property chart, indicating a family of selection guidelines for unspecified material properties, α and β.

1.3 Structural elements

The selection guideline is a function of the associated structural element under consideration. Structural components comprise many distinct structural elements, including ties, beams and plates (Figure 2). To simplify initial analysis, the pertinent geometry of each structural element can be represented by an associated free variable, resulting in material selection indices for the objectives of minimal mass and minimal cost (Table 1).

Each combination of structural element and associated free variable has a specific guideline gradient, k. The guideline gradient defines the relative contribution of the relevant material properties to performance (Figure 7):

- For $k \to \infty$, the selection guidelines tend towards vertical, and performance scales linearly with α. For minimal mass design, α represents the material density ρ, while for minimal cost design, α represents the cost per unit volume $C_m \rho$ (Table 1). Mass reduction scenarios with $k \to \infty$ benefit from a low density (or cost per unit volume for minimal cost design) in preference to a high fatigue strength.
- For $k \to 0$, the selection guidelines tend towards horizontal, and performance scales linearly with β. For fatigue-limited design, β represents material strength (Table 1). Mass reduction scenarios with $k \to 0$ benefit from a high material strength in preference to low density.
- For $k \in (0, \infty)$, performance is a compromise between these limiting scenarios.

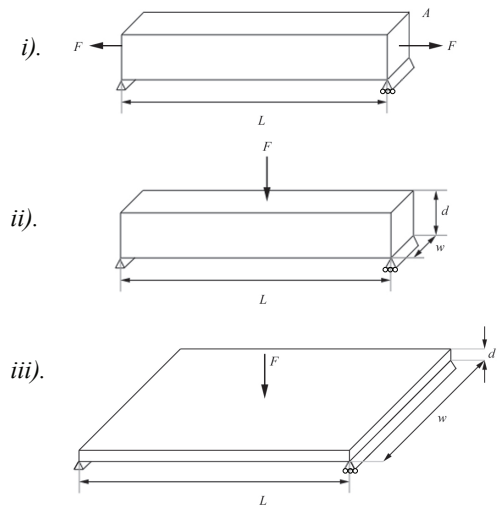

Figure 2. Simplified structural elements of relevance: tie (i), beam (ii) and plate (iii). Nomenclature: Force (F), Area (A), Length (L), width (w), depth (d).

Table 1.Material selection indices, including the free variable and guideline gradient, for strength-limited design of beam, tie and plate elements for minimal mass and minimal cost. Nomenclature: material density (ρ), material cost per unit mass (C_m), strength (S), Area (A), width (w), depth (d), material index (M^*_{kn}) The first suffix of a material index is the guideline gradient (k), the second suffix refers to the design objective, either minimal mass (m) or minimal cost (c).

				Objective	
		Free variable	***k***	**Minimal mass**	**Minimal cost**
Structural element	**Tie**	A	1	$M^*_{1m} = \left(\frac{\rho}{S}\right)$	$M^*_{1c} = \left(\frac{C_m\rho}{S}\right) = C_m M^*_{1m}$
	Beam	w			
		$A\ (w = d)$	3/2	$M^*_{3/2m} = \left(\frac{\rho}{S^{2/3}}\right)$	$M^*_{3/2c} = \left(\frac{C_m\rho}{S^{2/3}}\right) = C_m M^*_{3/2m}$
		d	2	$M^*_{2m} = \left(\frac{\rho}{S^{1/2}}\right)$	$M^*_{2c} = \left(\frac{C_m\rho}{S^{1/2}}\right) = C_m M^*_{2m}$
	Plate	d			

A beam or plate with depth as the free variable has the largest guideline gradient of the material selection indices of interest, i.e. $k = 2$. Materials employed in this scenario benefit more from low density than for any of the other material selection indices of interest (Table 1). Material selection indices with decreasing k are: beam with area as the free variable ($k = 3/2$); or, beam or tie with width or area as the free variable, respectively ($k = 1$). These elements increasingly benefit from high material strength in preference to low density for minimal mass design (or low cost per unit volume $C_m\rho$, for minimal cost design).

2 COMPONENT OVERVIEW

The component assessed is a linear actuator consisting of a DC motor, gear box and integral housing (Figure 3). The component provides linear actuation in a range of automotive applications, especially those associated with human and machine interfaces, such as the seat and steering wheel assemblies. The actuator may be used as a structurally loaded member that must meet service needs during typical use, as well as providing safety-critical crash performance. The form of the actuator is constrained by functional requirements, contribution to vehicle mass, initial cost and crashworthiness.

Opportunity may exist to enhance functional attributes (such as initial cost and mass) of an existing linear actuator, through the application of alternative material selection and structural shape optimisation. The following work assesses these possibilities. A research program was commissioned to:

1. Experimentally establish the properties of the existing component
2. Identify candidate materials
3. Suggest alternative component design structurally optimized for new candidate material

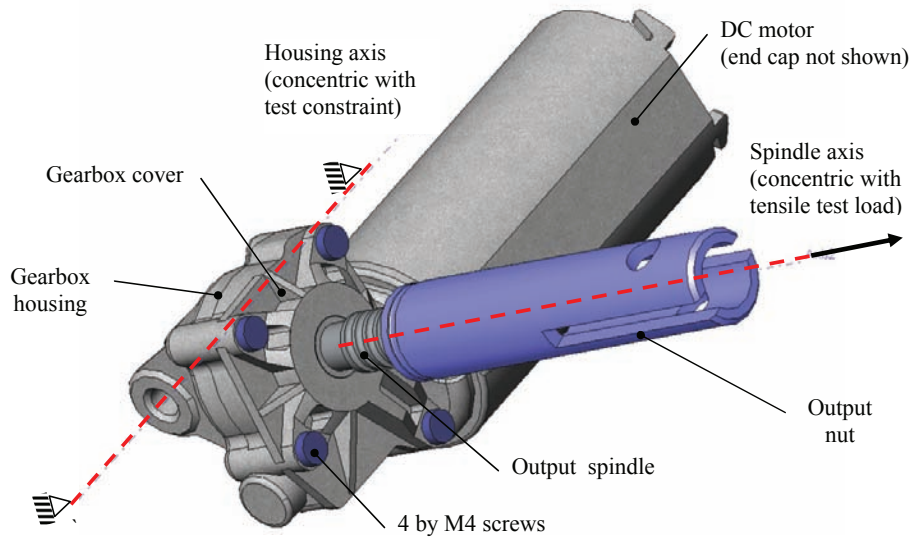

Figure 3. Linear actuator assembly

2.1 Actuator failure criteria

Assessment of actuator structural design is conducted according to its expected crash performance due to the peak loads experienced under a crash event. Crashworthiness is evaluated internationally by a range of standards, for example [4]. These standards include simulated accidents with various impact parameters. Two categories of impact scenario are of particular interest.

1. Low-speed impact is typically defined to occur in the range of 15-20 km/h. In addition to providing occupant protection, it is desirable that the actuator remain functionally and structurally uncompromised after a low speed-impact in order to avoid replacement. Plastic deformation of the actuator is the failure criterion for the low-speed scenario.
2. High-speed impact is typically defined in the range of 50-65 km/h. High-speed impact requires significant energy transfer and a very high potential for harm to the vehicle occupants. Plastic deformation is allowable, and desirable, for high-speed impact in order to minimize potential injury to occupants. Loss of functional integrity is allowable. Loss of structural integrity is the failure criterion for high-speed impact.

The scope of this work is to assess the optimisation opportunities associated with the low-speed impact scenario.

3 EXPERIMENTAL ANALYSIS

To obtain an understanding of the structural behavior of the linear actuator under investigation, an experimental study was conducted. The experimental stage subjected the complete linear actuator to tensile testing to obtain an indication of its method of failure and identify opportunities for design improvement within specific sub-components.

3.1 Initial testing

Tensile testing was carried out using a calibrated 50 kN capacity tensile test apparatus with an extension rate of 5mm/minute (Figure 4). Quasi-Static testing of this type provides a conservative basis for assessing the yield strength under dynamic (impact) conditions, as metallic materials display an increase in yield strength with increasing strain rate [5].

The actuator was constrained in the radial direction through the housing axis, and loaded in tension along the spindle axis (Figures 3 and 4). To allow for batch variation, actuators were collected from production seat assemblies over an extended time period. The resulting load extension curves are plotted in Figure 5. In addition to the extension of the actuator assembly, the indicated extension includes extension of the restraining bolts. Plastic deformation was observed in the restraining bolts (which contributes to the indicated extension). However, as the load path is in series, yield and peak load values are absolute. Further discussion of the influence of static and dynamic effects is provided in Section 2.1.

Multiple failure modes of the actuator assembly were observed (Table 2 and Table 3). Tensile testing was continued until at two failures were identified at each observed failure mode. There is little variance associated with the failure load of each mode (Table 2), and all failures occur within the range of 19.2±1.5 kN. This outcome suggests a highly robust design of the actuator sub-components, resulting in a lightweight cost efficient assembly. The lowest observed failure load corresponds to fracture of the gearbox cover at approximately 17 kN. Due to this observed discrepancy, the gearbox cover was selected as the focus of subsequent testing and design optimization.

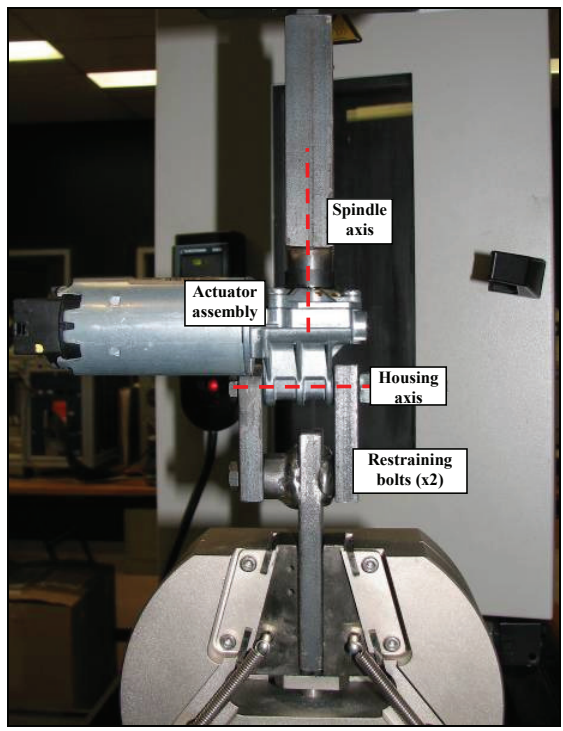

Figure 4. Complete actuator tensile test arrangement.

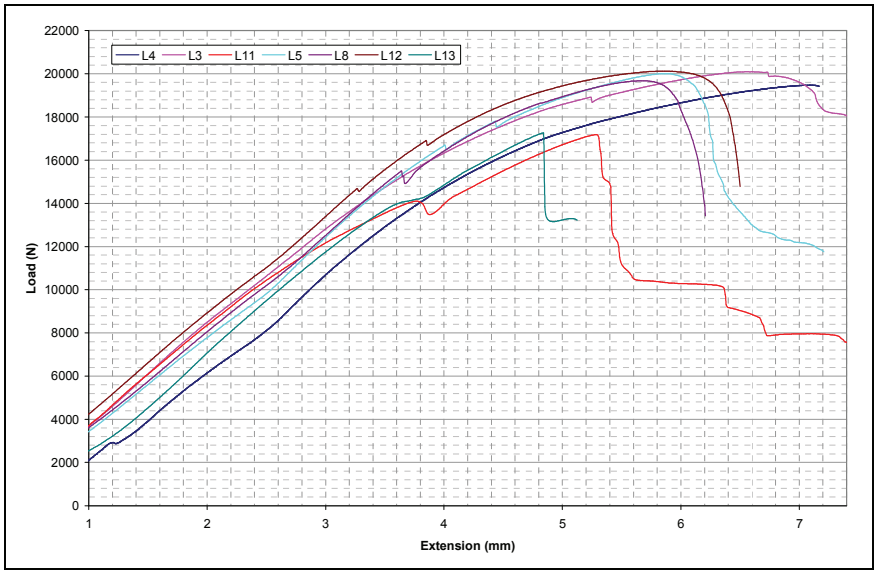

Figure 5 – Force-Extension curves for actuator assembly

Table 2 - Initial tensile test results.

Specimen ID	Maximum Load (kN)	Failure Mode
L 3	20.10	Fracture of gearbox housing
L 5	20.00	Fracture of gearbox housing
L 11	17.18	Fracture of gearbox cover
L 13	17.28	Fracture of gearbox cover
L 8	19.68	Worm tear out from plastic gear
L 12	20.12	Worm tear out from plastic gear

3.2 Material identification

The material and manufacturing processes associated with the housing cover were estimated by inspection to be HPDC zinc, due to the high geometric complexity, density [6] and the presence of ejector marks. This estimate was confirmed by assessing the material density and hardness, which corresponds to the range associated the Zinc-Aluminum Die-Casting Alloy AG40A (Figure 6).

4. MATERIAL SELECTION

An opportunity for design improvement through material substitution in the actuator housing cover was identified. To formally assess the opportunity for mass reduction the material selection procedures of Section 1 have been applied to identify candidate materials. A commercially available material selection tool [7] has been applied to a database of material types to systematically identify candidate material types and rank their relative performance.

An initial filter was applied to identify materials compatible with the intended method of manufacture, HPDC. Of the 64 material classes available in the material database, copper, magnesium, zinc lead and aluminum were found to be feasible with HPDC. Tensile yield strength was identified as the failure criteria for the low speed impact scenario. A series of material selection charts were developed to assist material selection for tensile strength. The material selection charts indicate the potential range of material properties associated with the feasible material classes for the design objectives of minimal mass and cost. Material selection guidelines are indicated for the scenarios identified in Section 1, i.e. k = 1, 3/2 and 2 (Figure 7).

Table 3. Failure modes of initial tensile test.

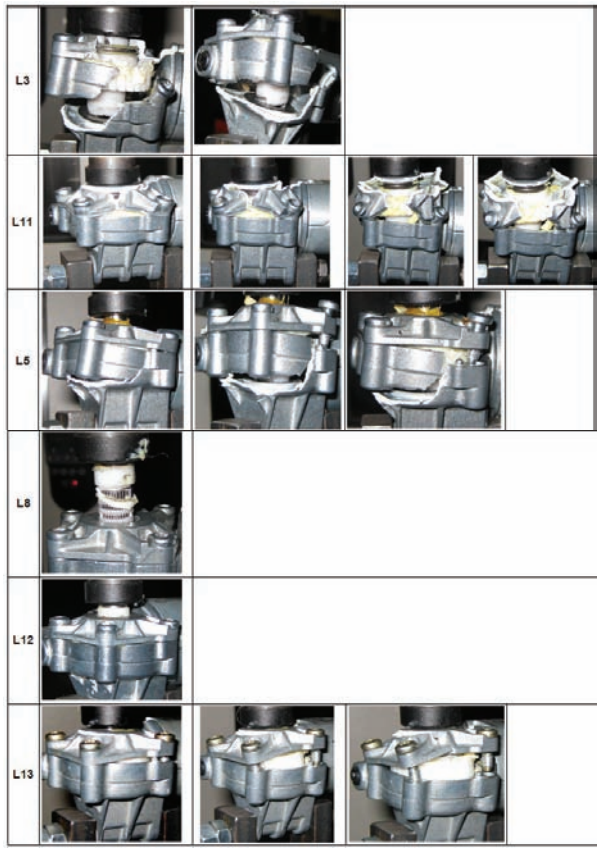

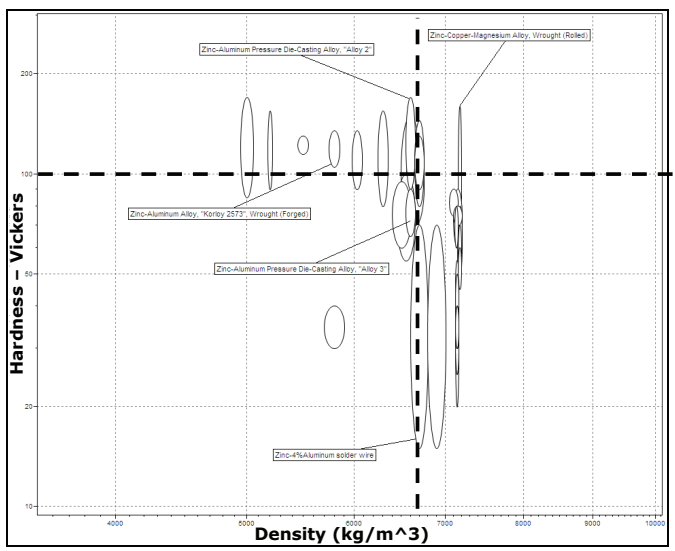

Figure 6. Density versus Hardness for a range of zinc alloys.

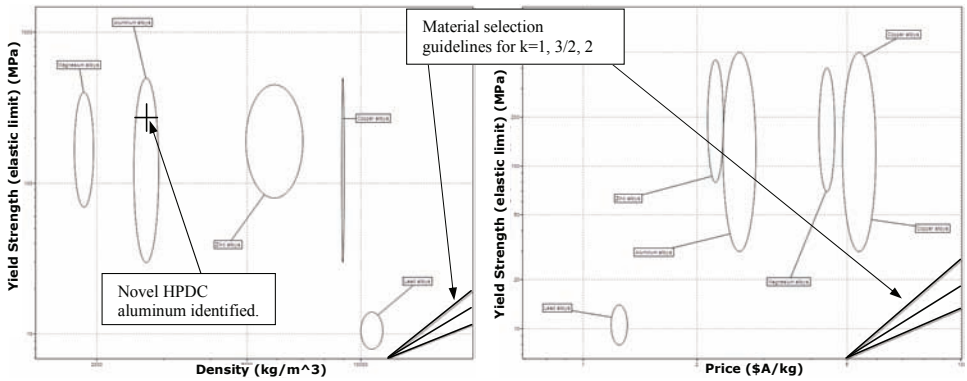

Figure 7. Yield strength versus density (left) and yield strength versus price (right). A cross indicates the position of the novel HPDC of Section 2.4.

The gearbox cover under investigation may be represented by a centrally loaded plate with perimeter supports (Figure 2), i.e. $k = 2$ (Table 1). By identifying the range of material selection indices achievable for $k = 2$ for each material class, a whisker-plot can be generated to indicate the potential benefits of material selection for the material classes feasible with HPDC (Figure 8). In summary, of the material classes:

- magnesium provides the lowest mass, but has the greatest associated cost penalty
- zinc provides the lowest cost
- aluminum may provide an opportunity to compromise between the objectives of minimal mass and cost
- although feasible, lead and copper are non-optimal for the material selection indices of interest

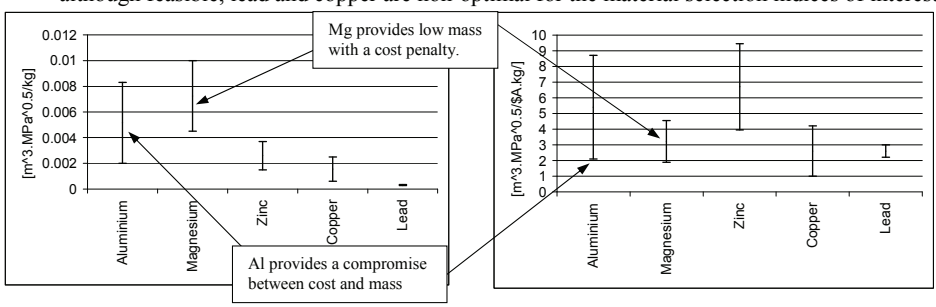

Figure 8. Whisker-plots indicating the potential range of material selection indices for k = 2 for material classes compatible with HPDC. Left: Minimal mass design, Right: Minimal cost design. Note material performance indices are defined according to [2].

2.4 Novel heat treatment of HPDC aluminum

HPDC aluminum alloys are not usually heat treated because the castings are relatively porous and contain entrapped gases. The associated pores expand during conventional solution treatment creating surface blisters, distortion and lower mechanical properties. Recent work has revealed a truncated solution treatment cycle that avoids these problems for HPDC aluminium alloys, allowing the yield stress to be approximately doubled when compared to the as-cast condition, [8]. The novel material is compatible with HPDC components ranging from small complex parts up to bulk components such as automotive transmission housings and engine blocks [9].

Aluminum has been identified as robust substitute material that provides a compromise between the objectives of mass and cost. The novel HPDC aluminum provides an opportunity to further improve the cost effectiveness of aluminum, and will form the basis for the ensuing optimisation. The preferred aluminum alloy selected for further investigation is A380 in the T64 Temper, due to the attractive balance of yield and tensile strengths combined with high fracture toughness.

4. OPTIMIZATON

An opportunity for design improvement through material substitution in the actuator gearbox cover was identified in the preceding sections. The candidate materials offer higher yield strength and lower mass than the ZnAl alloy currently used and permit a more efficient housing cover topology to be utilized. To identify an optimized topology, a parameterized Finite Element (FE) model of the housing cover was constructed and a structural optimisation problem formulated.

4.1 Finite Element Model

A parametric FE model of the upper housing cover was constructed in CATIA CAE software (Figure 9). The model consisted of approximately 11 000 3D parabolic tetrahedral elements with 20 000 corresponding nodes. The model was analysed for the case when the actuator assembly is subjected to tensile load (Figure 4). Actual loading conditions experienced by the housing cover were simulated by applying rigid restraints to the four screw holes and a distributed load on the back cap face as shown in Figure 9. A load of 3 kN was found to correspond to an estimated stress in excess of the lower bound of the material yield strength reported for AG40A material (i.e. 140 MPa). The identified load was used as the reference load in the subsequent structural optimisation problem.

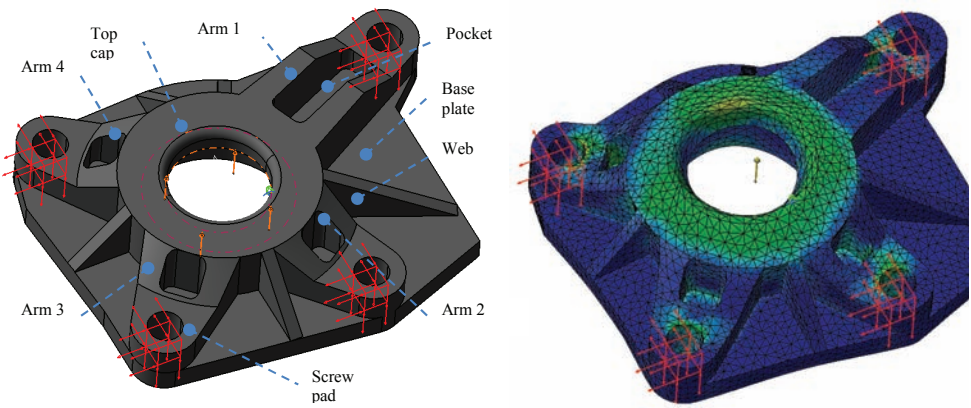

Figure 9. Model of original cover geometry (left) and stress distribution (right).

In order to improve parameterization of the model for the optimisation process, modifications were made to reduce model complexity. Upon initial examination of the stress distribution in the original housing cover (Figure 9), it was noted that the existing stiffening webs may be removed without adverse effect as they add little to the strength to the structure. A minor modification was also made to the slanting portion of the stiffening arm geometry, where the original revolved cut was replaced with a taper and two fillet radii at intersections with the top face and the screw pad, respectively (Figure 10). When subjected to the reference load, the maximum stress of 138 MPa in the original model occurred on the inside back face of the top cap. In the modified model the peak stress was 143 MPa and occurred in the same zone. This result suggests the modified model is a close analogue for the original. The modification improves the potential for parameterizing and has only minor influence on the nature of the stress distribution.

Figure 10. Model of modified cover geometry (left) and stress distribution (right).

4. 2 Methodology

A multi-objective optimisation problem was formulated by interfacing a parametric FE CATIA model with modeFRONTIER optimisation software with the objectives of minimal mass and peak stress subject to the identified reference load. The material properties used in the analysis were those of the new candidate material (A380-T64). The candidate material has a significantly higher yield stress than the existing zinc material (270MPa versus 140 MPa) and lower density (2.7 g/cm^3 versus 6.7 g/cm^3).
The allowable stress was limited to the yield strength of the preferred aluminum alloy, A380-T64 (270 MPa). The mass of the housing cover of original geometry, but with material density corresponding to A380-T64 was set as the mass limit (18g).
The optimization methodology consisted of applying a multi-objective Genetic Algorithm (GA) to a randomly initialized population of parameter values and searching for a set of optima. A genetic algorithm was selected for this work as such techniques have proven effective in similar structural optimisation problems [10]. Genetic algorithms are popular optimization algorithms developed to mimic the processes of evolutionary biology [11]. A random population of input variables was coded into binary *string* structures. The strings are subsequently evaluated to identify their associated *fitness*, a measure of how well objectives are satisfied. The population of individuals is then improved through manipulations that are analogues for the mechanics of natural selection. The outcome is a new, superior population of strings, which once again is evaluated for fitness and manipulated. Multiple iterations, or *generations*, of the process are carried out until a termination requirement is passed, for example the number of generations. The outcome is hopefully a superior combination of variables that better satisfy the problem objectives.

4.3 Results

The modified housing cover used for optimisation consists of 11 geometric parameters. A population of 70 variables was initialized using a Sobol quasi-random sampling algorithm, and subjected to a GA of 50 generations giving a total of 3,500 design evaluations. A Sobol sampling algorithm was selected as it provides improved uniformity in filling the design space when compared to a randomly generated sequence [12]. The optimization problem parameters, initial values, and optimized results are presented in Table 4. The associated design space, i.e. all evaluated deigns, is identified (Figure 11).
Out of the evaluated deigns, a global optimum was identified which minimises the housing cover mass without violating stress constraints (Figure 12). A number of more conservative designs were also identified. Design 3188 (Figure 13) was selected as a good compromise between the objectives and providing some design conservatism by not approaching too close to the yield stress boundary.

4. CONCLUSION

An opportunity for design improvement through material substitution was identified by experimental assessment of an existing linear actuator. Traditional material selection procedures were applied to screen a broad database of materials to identify feasible candidates and to quantify their relative merit. For the plate structural element, aluminum was identified as robust substitute material that provides a compromise between the objectives of mass and cost and may provide an opportunity for enhanced material selection. Further assessment by numerical methods identified additional opportunities for topological optimisation.
A novel process, patented by CSIRO Australia, allows heat treatment of HPDC aluminum alloys and offers higher yield strength and lower mass than the in the as-cast condition. Further work associated with this project includes the quantification of the specific costs associated with the heat treated HPDC alloy, and experimental verification of results.
Traditional material selection tools are able to engage with a large number of candidate materials, but provide little design guidance for the optimisation of a specific scenario. Numerical optimization provides deep insight into specific scenarios, but incurs a significant computational cost. The material selection and optimisation technique applied in this paper provides an example of the efficient integration of both methods; i.e. a course filter is applied to rapidly screen a large database of candidates, resulting in an identified subset that can be processed by the numerical methods within available design time.

Table 4 – Optimization parameters and results

PARAMETER	DESCRIPTION	ORIGINAL HOUSING COVER	INITIAL MODIFIED MODEL	OPTIMAL MODIFIED MODEL (CONSERVATIVE)	OPTIMAL MODIFIED MODEL (MIN. MASS)	LOWER BOUND	UPPER BOUND
Material	Housing cover material	ZnAl Alloy (AG 40A)	Al Alloy (A380 T64 Temper)			-	-
T_p	Base plate thickness	2.5 mm	2.5 mm	1.5 mm	1.5 mm	1.5 mm	5 mm
T_c	Top cap thickness	2.5 mm	2.5 mm	2.67 mm	1.89 mm	1.5 mm	5 mm
T_{wall}	Top cylinder wall thickness	2 mm	2 mm	1.5 mm	1.5 mm	1.5 mm	5 mm
H_{pad}	Screw pad recess	3.2 mm	3.2 mm	3 mm	3 mm	1 mm	5 mm
$W_{pocket\ 1}$	Arm 1 pocket width	4.8 mm	4.8 mm	5 mm	5 mm	2 mm	6 mm
$W_{pocket\ 2}$	Arm 2 & 3 pocket width	4.8 mm	4.8 mm	5 mm	5 mm	2 mm	6 mm
$W_{pocket\ 3}$	Arm 4 pocket width	4.8 mm	4.8 mm	5 mm	5 mm	2 mm	6 mm
A_1	Sweep angle of arm 1	10 deg.	10 deg.	2 deg.	2 deg.	2 deg.	24 deg.
A_2	Sweep angle of arm 2	20 deg.	20 deg.	2 deg.	2 deg.	2 deg.	30 deg.
A_3	Sweep angle of arm 3	20 deg.	20 deg.	6 deg.	2 deg.	2 deg.	30 deg.
A_4	Sweep angle of arm 4	20 deg.	20 deg.	18.28 deg.	2 deg.	2 deg.	40 deg.
V	Housing cover volume	6.57 cm^3	6.50 cm^3	5.18 cm^3	4.60 cm^3	-	6.50 cm^3
m	Housing cover mass	47 g	18.5 g	14.1 g	12.47 g	-	19g
σ_{max}	Maximum stress	138 MPa	143 MPa	172.38 MPa	264.32 MPa	-	270 MPa
Design ID	Design reference number	0	1	3188	2194	-	-

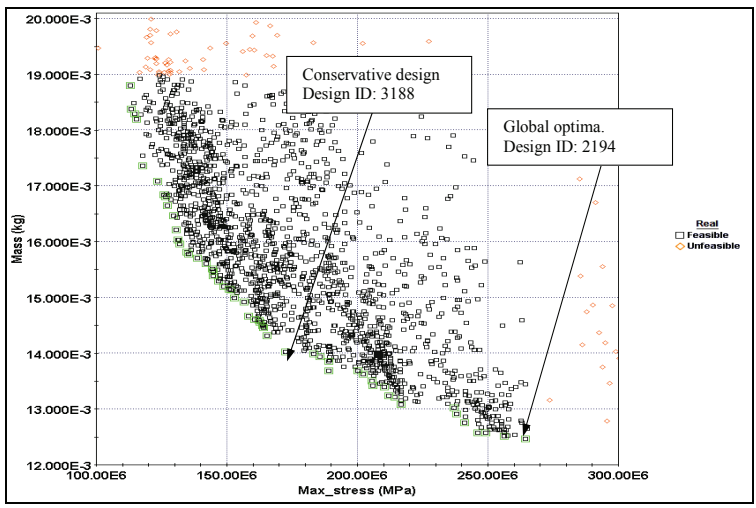

Figure 11 – Design Space. Design ID associated with Table 4 identified.

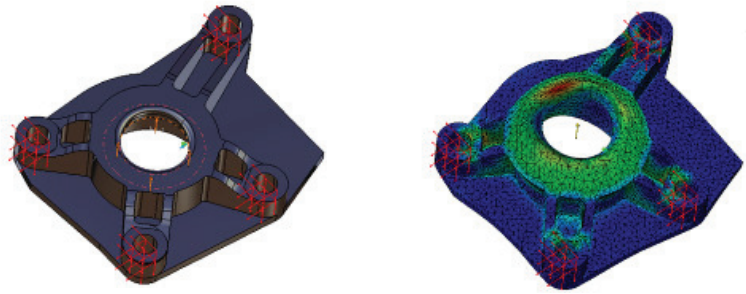

Figure 12. Global optimum design #2194

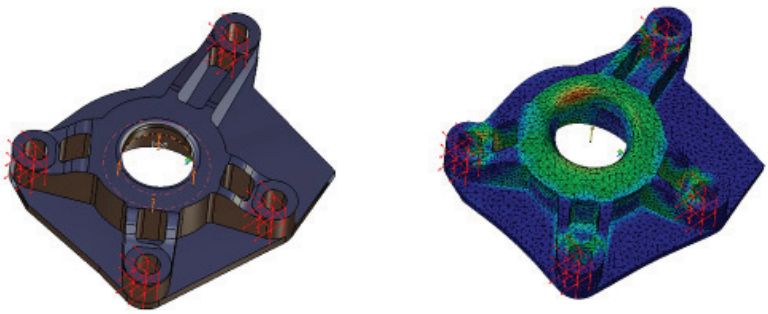

Figure 13. Conservative Design #3188

REFERENCES

1. Crane, F.A.A. and J.A. Charles, *Selection and Use of Engineering Materials*. 1984.
2. Ashby, M., *Multi-Objective Optimization in Material Design and Selection.* Acta Materialia, 2000. **48**(1): p. 359-371.
3. Ashby, M., *Material Selection in Mechanical Design (Volume III)*. Third ed. 2005: Butterworth Heinemann, UK.
4. United States Government Accountability Office, *Report to Congressional Committees. Vehicle Safety. Opportunities Exist to Enhance NHTSA's New Car Assessment Program.* 2006. p. 124.
5. Shigley, J.E., *Mechanical Engineering Design*. 1986: McGraw Hill.
6. Schey, J.A., *Introduction to Manufacturing Processes*. 1999: Mcgraw-Hill.
7. Cebon, D., M. Ashby, and L. Lee-Shothaman, *Cambridge Engineering Selector v4 User's Manual*. 2002, Cambridge UK: Granta Design Limited.
8. Lumley, R.N., et al., *Heat Treatment of High Pressure Diecastings.* Metallurgical and Materials Transactions A, 2007. **38A**: p. 2564-2574.
9. Lumley, R., *Automotive Weight Reduction Through the Use of High Strength Aluminium Diecastings*, in *Proc. International Conference on Sustainable Automotive Technologies*, A. Subic, M. Leary, and J. Wellnitz, Editors. 2008.
10. Coley, D., *Genetic Algorithms - An Introduction for Scientists and Engineers*. 1999, Singapore: World Scientific.
11. Deb, K., *Optimization for Engineering Design* 2006, New Dlhi: Prentice-Hall.
12. Sobol, I., *Uniformly Distributed Sequences with an Additional Uniform Property* 1977. **16**(USSR Computational Mathematics and Mathematical Physics): p. 236-242.